Hydrogen Recombination in Natural Masing

Samantha Powers

under the direction of
Prof. Edmund Bertschinger and Mr. Phillip Zukin
Department of Physics
Massachusetts Institute of Technology

Research Science Institute
July 31, 2007

Abstract

The conditions necessary to produce natural hydrogen recombination masers are not fully understood. To explore the requirements, we simulate the recombination of a plasma cloud, only tracking the evolution of two bound states. We modify the principle quantum number and angular momentum of the bound states, as well as the temperature and density of the cloud, to pin down what effect each has on masing. The angular momentum value primarily determines when masing occurs, but density, temperature, and principle quantum number also play a role.

1 Introduction

A decade after lasers had been created in the laboratory—and half a century after they had been theorized—it was discovered that light of unusual intensity could be emitted by astrophysical sources. The hydroxyl radical, water, and silicon oxide, amongst other compounds, were found to frequently produce strong lasing but hydrogen, the most common element and the simplest to model, was not. The reason for this is not well understood, and this paper seeks to explore the conditions under which lasing occurs naturally in hydrogen gas.

A simple three level model is simulated with a system of ordinary differential equations. Using a series of realistic initial conditions, this system is solved to establish conditions that could theoretically produce a laser.

1.1 Laser Theory

The fundamental component of lasers is the gain medium, in which the light is generated. When energy—a pulse of light, for example—is applied to the medium, some of the electrons in the atoms will be promoted to a higher energy level, making the atoms excited.

The excited atom is not stable, so eventually an electron will spontaneously fall back down to a lower energy state, releasing a photon. This photon travels through the medium, eventually intercepting another atom. If the atom is excited, the perturbation caused by the electric field of the wave may knock the electron back to its ground state, causing a wave of light of equal wavelength and phase to be released in the same direction as the first. This process is called stimulated emission. Now there are two waves where once there was one, each of which may intercept another atom to begin the chain reaction.

When the light produced is in the microwave range, the system is called a maser - microwave amplification by stimulated emission of radiation.

There must be enough excited atoms through which the light can be amplified for the

system to become a maser. When there are more atoms of a higher energy than there are those of a lower, a population inversion exists that is sufficient to satisfy this condition. The models described in this paper are created with the goal of simulating a population inversion, for the purpose of discovering how it may be achieved in clouds of atomic hydrogen.

If the upper level population is constantly being renewed, the population inversion is maintained, and lasing can occur continuously. The light produced in this way is called a continuous wave. The method of replenishing the upper population is called the pumping mechanism. In astronomical masers, the pumping mechanism is often a nearby star of sufficient energy to excite or ionize the atoms. Once the atoms have been ionized, recombination can take place.

Hydrogen recombination occurs when an electron is captured by a proton. It favors changes of greater energy—the greater the energy released, the higher the rate of recombination to that energy level. Relative recombination rates are discussed in more detail later.

1.2 MWC 349

MWC 349A, part of the binary star MWC 349, is the only known natural hydrogen recombination maser. It produces nine masers, and amplifies weakly at other wavelengths. The transitions involved in the strong masing include H15α, H12α, and H10α [6]—the number in the notation is the lower level, and the α indicates that the transition is between adjacent levels.

The cloud surrounding MWC 349A is ionized and resembles a butterfly in shape [2]. There is evidence to suggest it acts like a Keplerian disk seen edge on [2, 3], which means it rotates faster at smaller radii. Doppler shifting changes the frequency of the light such that photons produced in one part of the cloud will not be of the right frequency to stimulate emission in atoms from another part of the cloud, if they are moving at different speeds.

Therefore only rings of gas, all moving at the same speed, will be able to lase, and we will only be able to observe masing that occurs in our direction. So for any given ring there are two areas of masing—the part of the ring moving away from us produces light that is red shifted, and the part moving towards us produces blue shifted light, producing a double-peaked spectrum [2].

It has also been suggested that masing can occur in high enough density clouds of ionized hydrogen, but this situation has never been observed [4, 6].

2 Creating the Model

The hydrogen model has been simplified to two bound levels, an upper state, indicated by u with population density N_u, and a lower state, indicated by l with population density N_l. The population of the continuum, which contains unbound electrons and protons, is also considered and can be calculated by subtracting the populations of the bound levels from the total proton number, given by N_t. The proton population of the continuum is represented by N_p.

$$N_p = N_t - N_u - N_l$$

There are a few things to consider about level choice: the lower state can be the ground state, but the recombination rate to the ground state is high and does not encourage a population inversion. On the other hand, the photon released by recombination to the ground state has enough energy to ionize any atom absorbing it so there is no net change in the ground state population if the absorption rate is high. Nevertheless, it is expected that transitions between higher states will more readily produce an inversion. For simplicity's sake, this paper will ignore this photoionization factor and instead focus on the case where the system was ionized to begin with—this is called the pure recombination case.

The model is a system of differential equations, designed to take into account three main

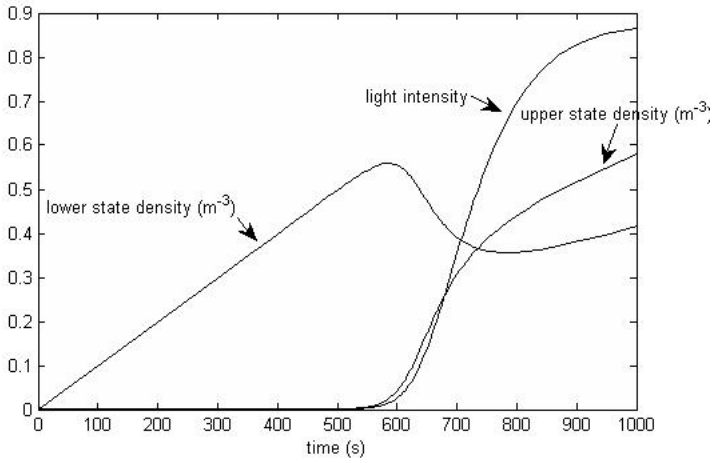

Figure 1: Example of an inversion

dynamic rates: the change in the population of the lower state, the change in the population of the upper state, and the change in the intensity of the light the maser is producing. The latter tracks the population of photons with the energy of the difference between the upper and lower states. A dramatic increase in this population signals that masing has occurred, shown in Figure 1. A consistently high intensity indicates that a pumping mechanism is repopulating the upper state. A momentary spike indicates that the population inversion could not be maintained.

There are five major radiative processes that change the number of atoms of a particular excitation state: absorption of a photon, ionization (which we are ignoring), spontaneous and stimulated emission of a photon, and recombination.

To calculate the number of excited atoms as a function of time, all processes that might increase or reduce the population must be taken into account. First, absorption of a photon of sufficient energy by a ground state atom will increase the number of excited atoms. Absorption of a sufficiently energetic photon by an already excited atom will allow the electron to escape, thus reducing the number of excited atoms. Spontaneous or stimulated emission of a photon will reduce the excited population, and recombination will increase it (see Table

1 for specifics. A is the Einstein A-coefficient between the upper and lower levels. Since in this simplified model we are ignoring photoionization, $n_{\gamma l}$ and $n_{\gamma u}$ are assumed to be zero.

Name	Ground Change	Excited Change	Factor
absorption	-	+	$A\frac{gl}{gu}N_l n_\gamma$
ionization: g	-	0	$\frac{4\pi\sigma_u \nu u^3}{c^2}N_l n_{\gamma l}$
ionization: e	0	-	$\frac{4\pi\sigma_u \nu u^3}{c^2}N_u n_{\gamma u}$
stim emiss	+	-	$AN_u n_\gamma$
spont emiss	+	-	AN_u
recomb: g	+	0	$\alpha_l N_e^2$
recomb: e	0	+	$\alpha_u N_e^2$

Table 1: To calculate population change, locate the appropriate column, apply the sign given to the factor, and sum.

Thus, we produce the equation

$$\frac{dN_u}{dt} = A\frac{g_l}{g_u}N_l n_\gamma - AN_u n_\gamma - AN_u + \alpha_u N_e^2 - \frac{4\pi\sigma_u \nu_u^3}{c^2}n_u n_{\gamma u}.$$

where N_u represents the population density of the upper excited state, N_l represents population change for the lower state, and c stands for the continuum. Appendix A contains the other constant/variable definitions and derivations.

The same type of equation can be formed for N_l

$$\frac{dN_l}{dt} = -A\frac{g_l}{g_u}n_l n_\gamma + AN_u n_\gamma + AN_u + \alpha_{cl} N_e^2 - \frac{4\pi\sigma_l \nu_l^3}{c^2}N_l n_{\gamma l}.$$

Assuming conservation of protons and electrons, N_e and N_p can be calculated. In fact, if the system is neutral, $N_e = N_p$.

The radiative transfer equation, equation 1, which describes the photon distribution function $f(v, s)$, takes into account the stimulated emission factor $\frac{N_u}{g_u}$, the absorption factor $\frac{N_l}{g_l}$, and the spontaneous emission factor $\frac{N_u}{g_u}$. Stimulated emission and absorption both depend on the current photon distribution, so both are multiplied by f, whereas spontaneous

emission does not. It should be noted that equation 1 is given in terms of s, or path length, but can be converted to t using the speed of light as needed.

$$\frac{df}{ds} = \frac{c^2 g_u A}{4\pi\nu_0^2}\phi(v)\left(\left(\frac{N_u}{g_u} - \frac{N_l}{g_l}\right) f(v,s) + \frac{N_u}{g_u})\right) \tag{1}$$

Equation 1 can be redefined as

$$\frac{df}{ds} = -k_\nu f + j_\nu,$$

where k_ν and j_ν are defined as:

$$k_\nu = \frac{c^2 g_u A}{4\pi\nu_0^2}\phi\left(\frac{N_l}{g_l} - \frac{N_u}{g_u}\right)$$

$$j_v = \frac{c^2 g_u A}{4\pi\nu_0^2}\phi\frac{N_u}{g_u}.$$

However, there is a spread to the maser line, which is not taken into account by the function $f(\nu, s)$. One must multiply $f(\nu, s)$ by the Lorentzian line shape function $\phi(\nu)$ 2 and integrate for all positive ν, to get n_γ 3.

$$\phi(\nu) = \frac{A/2\pi}{(\nu - \nu_0)^2 + (A/2)^2}, \tag{2}$$

$$n_\gamma = \int_0^\infty \phi(\nu) f(\nu, s) d\nu. \tag{3}$$

By differentiating, one gets:

$$\frac{dn_\gamma}{ds} = \int_0^\infty [-k_\nu f + j_\nu] = -K n_\gamma + J,$$

where

$$K = \int_0^\infty k_\nu \phi(\nu) d\nu = \frac{c^2 g_u A}{4\pi}(\frac{N_u}{g_u} - \frac{N_l}{g_l})\frac{\int_0^\infty \frac{\phi^2(\nu)}{\nu_0^2} f(\nu, s) d\nu}{\int_0^\infty f(\nu, s)\phi(\nu) d\nu},$$

$$J = \int_0^\infty j_\nu \phi(\nu) d\nu = \frac{Sc^2 g_u A}{4\pi} \frac{N_u}{g_u} \int_0^\infty \frac{\phi^2(\nu)}{\nu_0^2} d\nu.$$

In unsaturated masers, whose level populations change slowly, k_ν and j_ν are essentially constant and $f(\nu, s)$ can be evaluated exactly. However, to compute K, an approximation of $f(\nu, s)$ can be made to simplify the expression, using the first two terms of the Taylor polynomial for e on the assumption that $k_\nu s$ is close to 0. This gives

$$\int f(\nu, s)\phi(\nu) d\nu = \frac{sc^2 g_u A}{4\pi v_0^2} \frac{N_u}{g_u} \int \phi^2(\nu) d\nu.$$

Solving for $f(\nu, s)$ exactly gives $f(\nu, s) = \frac{j_\nu}{k_\nu}(1 - e^{-k_\nu s})$ if one assumes $f = f_0(\nu)$ at $s = 0$ and $f_0(\nu) = 0$. The form can be generalized, assuming $f_0(\nu) = d$, to

$$n_\gamma(s) = n_\gamma(0)e^{-ks} + \frac{j}{k_\nu}(1 - e^{-k_\nu s}).$$

Mathematica was used to find the definite integrals of $\phi^2(v)$ and $\phi^3(v)$, which were then evaluated from 0 to ∞.

$$\int_0^\infty \phi^2(\nu) d\nu = \frac{1}{A\pi^2}(\frac{\pi}{2} + \frac{2A\nu_0}{A^2 + 4v_0^2} + \arctan(\frac{2\nu_0}{A})),$$

$$\int_0^\infty \phi^3(\nu) d\nu = \frac{1}{2A^2\pi^3}(\frac{3\pi}{2} + \frac{2A(5A^2 + 12(\nu_0)^2)\nu_0}{(A^2 + 4(\nu_0 - \nu)^2)^2} + 3\arctan(\frac{2\nu_0}{A})).$$

In all cases in which we are concerned, A is small compared to ν_0, so when they are added A disappears. The Taylor expansion of the arctangent term approaches $\pi/2$, and the equations simplify to

$$J(s) = \frac{c^2 N_u}{4\pi^2 v_0^2},$$

$$K(s) = \frac{3c^2 g_u}{8\pi^2 v_0^2}.$$

However, these terms put our equations in terms of path length, s. To change from arclength to time in seconds, the terms must be multiplied by ct.

By inputting specific initial values into these equations, the population levels can be calculated over time using MatLab, and it can be determined whether or not the system with those values will lase.

2.1 Data Collection

To determine whether a population inversion occurs, we graph $k_\nu s$ over time to see if the value ever becomes negative. If it never does, the graph was deemed non-masing. If it did, a population inversion had been created.

Recombination coefficients and spontaneous emission coefficients for each n and l tested are included in Appendix B.

2.1.1 First variation: l value

The angular momentum quantum number, or l value, of an electron represents the shape of the orbital it inhabits. The value ranges from 0 to $n-1$, where n is the principle quantum number. When an electron move from one orbital to another, its l value must either increase or decrease by one.

To test how much l value variance affects results, we looked at the 10 to 11 transition at 10^4 K with a density of $10^9 m^{-3}$. Graphs showing typical inversion and non-inversion results are shown in figure 2.

For transitions where the l value of the upper state is one lower than the l value of the lower state, a population inversion occurs. For the other half of transitions, a population inversion does not occur. The trend also holds for higher transitions (15-16, 20-21, 25-26)

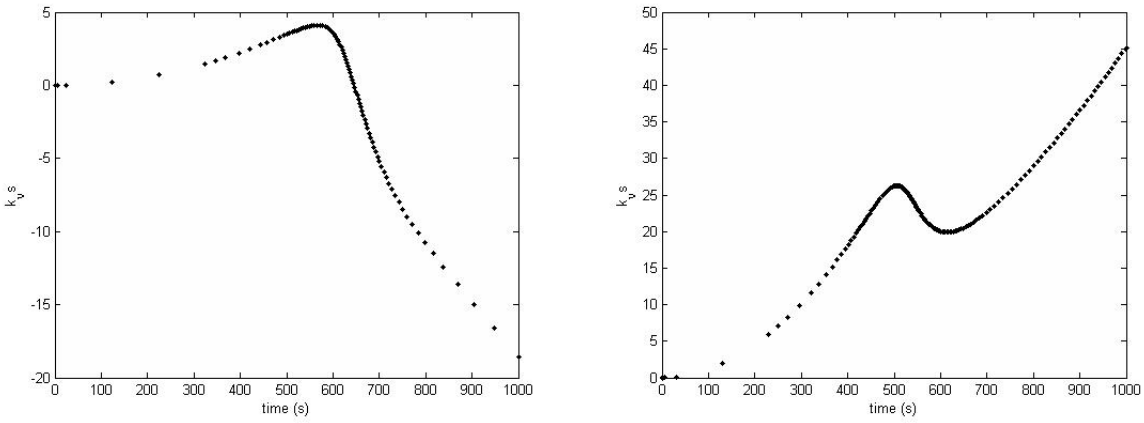

(a) Inversion

(b) Not an inversion

Figure 2: Example $k_\nu s$ graphs

where the l values chosen are roughly half of the n value.

There are a couple of caveats, though. The first is that we assume our maser is unsaturated, though this may not be the case at all times. Second, in our derivations we assumed $|k_\nu s|$ to be less than one. Unfortunately, it can be seen that $|k_\nu s|$ exceeds one at some point in every plot.

However, it is still the case that the spontaneous emission coefficient A, which is not derived with $k_\nu s$, is lower for the cases where the upper state l value is one less than the lower state l value. Spontaneous emission drains the upper level and repopulates the lower level, so a small A value increases the likelihood of a population inversion and reinforces the idea that the results we obtained are accurate.

Furthermore, on the whole, the α values—the recombination coefficients—are higher for the upper level than the lower level only for the l value cases described above. When the recombination rate is higher for the upper level than the lower, electrons fall more readily into the upper state and a population inversion is more easily achieved.

2.1.2 Second variation: n value

For configurations with high n values, the recombination coefficients cannot be calculated with the program we were using, which limits exploration of this variation.

Nevertheless, as n gets larger, A gets smaller, which, as mentioned above, indicates population inversion should be more likely. However, if the l value for the upper state is not one less than the l value for the lower state, the inversion still does not occur. This is probably because the recombination rate for the upper state is not higher than that of the lower state, which indicates that recombination rates are more influential in inverting the population than spontaneous emission rates are.

2.1.3 Temperature and Density

Recombination rates are affected by the temperature of the system, lower being more favorable for a population inversion, as well as the density, higher being more favorable. With this in mind, both temperature and density variation are explored.

10^3, 10^4, and 10^5 K were computed for $n = 10$, $l = 5$ to $n = 11$, $l = 4$ and $n = 10$, $l = 5$ to $n = 11$, $l = 4$. Interestingly, only 10^4 produces a higher recombination rate for the upper state than for the lower state, though the pattern of l transition states dominates — each case, no matter the temperature, where the upper state l value was lower than the lower state l value, produces a population inversion.

For density, because the recombination terms involve the square of the density while the other terms are only linearly dependent, an increase in density should cause the cases where the recombination rates of the upper state are higher to more readily experience population inversion. However, in all such cases, every density produces a population inversion, and a higher density only causes them to invert more quickly.

A faster inversion, whether the result of a low temperature or a high density, means a maser of higher intensity, or even a more likely maser in real situations where the size of the

gain medium is not unlimited.

3 Conclusion

We modeled a pure recombination hydrogen maser using a system of differential equations to represent the population of an upper excited state, the population of a lower excited state, and the intensity of the maser light produced. We varied the n and l values as well as temperature and density to establish the conditions under which masing would occur.

The trend indicates that a maser is produced in every case in which the upper state l value is one less than the lower state l value. A higher n value decreases the spontaneous emission rate but does not seem to create a population inversion in and of itself. Similarly, temperature modifies recombination rates but does not appear to be a deciding factor when the size of the gain medium is unlimited. Density too changes the rate at which inversion occurs.

Interestingly, every graph analyzed involved a permanent population inversion, despite the fact that no pumping mechanism was in place. It is possible that for the higher n values we could not calculate, a non-permanent increase in intensity would be created. It is also possible that the permanency of the intensity increase is due to the breakdown of our assumptions.

Further explorations will involve increasing the number of bound states, increasing the accuracy of the approximations, incorporating photoionization into the equations, and establishing a fixed size of the gain medium to determine what temperature and density combinations are feasible.

4 Acknowledgments

I'd like to thank Dr. Bertschinger for giving me this opportunity and for spending the copious amounts of time necessary to help me understand the core concepts of this project. I'd also like to thank Phillip Zukin for his patience and the time he took to make this project actually work with some amount of reliability. Thanks also go to Allison Gilmore and those who read my paper for helping me make it correct and understandable. Finally, I very much appreciate the experience that the Research Science Institute and Ms. DiGennaro have given me.

References

[1] Elitzur, Moshe. Astronomical Masers. Dordrecht, Netherlands: Kluwer Academic Publishers, 1992.

[2] Gordon, M. A. 1992, ApJ, 387, 701.

[3] Martin-Pintado, J., Bachiller, R., Thum, C., and Walmsley, C.M. 1989a, Astr. Ap., 215, L13.

[4] Spaans, M., & Normal, C. A. 1997, ApJ, 488, 27.

[5] Storey, PJ. "Programs in Physics & Physical Chemistry." Computer Physics Communications Program Library. 1990. Science Direct. 30 Jul 2007 <http://cpc.cs.qub.ac.uk/>.

[6] Strelnitski, V. , Haas, M.. R., Smith, H. A., Erickson, E. F., Colgan, S. W. J. & Hollenbach, D.J. 1996a, Science, 272, 1459.

A Appendix A

Var	Represents	Derivation/Source	Value	Units
ν_0	frequency: upper to lower	$10.2(eV) * 1.6 * 10^{-19}(J/eV)/h$	$2.46 * 10^{15}$	Hz
ν_1	frequency: to lower	$13.6(eV) * 1.6 * 10^{-19}(J/eV)/h$	$3.28 * 10^{15}$	Hz
ν_2	frequency: to upper	$3.4(eV) * 1.6 * 10^{-19}(J/eV)/h$	$8.21 * 10^{14}$	Hz
Tc	cloud temperature	case dependent	10000	K
n	proton density	case dependent	10^9	$1/m^3$
g_l	degeneracy of lower	$2l_l + 1$	depends	unitless
g_u	degeneracy of upper	$2l_u + 1$	depends	unitless
A	spontaneous emission coefficient	measured/calculated	$4.67 * 10^8$	1/s
α_l	recombination coefficient to lower	calculated	$2.28 * 10^{-13}$	m^3/s
α_u	recombination coefficient to upper	calculated	$8.33 * 10^{-14}$	m^3/s
K	intensity coefficient	$\frac{c^2 g_u A_{ul}}{4\pi}\left(\frac{N_u}{g_u} - \frac{N_l}{g_l}\right)\frac{\frac{1}{\nu_0^2 2A^2\pi^3}\left(\frac{3\pi}{2} + \frac{2A(5A^2+12\nu_0^2)\nu}{(A^2+4\nu_0^2)^2} + 3arctan\left(\frac{2\nu_0}{A}\right)\right)}{\frac{1}{A\pi^2}\left(\frac{\pi}{2} + \frac{2A\nu_0}{A^2+4\nu_0^2} - arctan\left(\frac{2\nu_0}{A}\right)\right)}$	varies	unitless
J	intensity term	$\frac{c^2 g_u A_{ul}}{4\pi}\frac{N_u}{g_u}\frac{1}{A\pi^2\nu_0^2}\left(\frac{\pi}{2} + \frac{2A\nu_0}{A^2+4\nu_0^2} + arctan\left(\frac{2\nu_0}{A}\right)\right)$	varies	unitless
$n_{\gamma 1}$	Photon occupation number for ν_1	approximation	***	unitless
$n_{\gamma 2}$	Photon occupation number for ν_2	approximation	***	unitless
dN_l/dt	Lower state population change	See Separate	...	$1/(m^3 * s)$
dN_u/dt	Upper state population change	See Separate	...	$1/(m^3 * s)$
dn_γ/dt	Change in photon occupation	$-Kn_\gamma + J$	...	1/s

Table 2: Variables/Constants in Use, calculations for ground and 1st excited

B Appendix B

lower n	lower l	upper n	lower l	Temperature(K)	lower α	upper α	A	masing?
10	1	11	0	10^4	7.81e-22	2.16e-22	1.36e4	y
10	1	11	2	10^4	7.81e-22	8.27e-22	1.16e4	n
10	5	11	4	10^4	6.52e-22	7.46e-22	2.00e3	y
10	5	11	6	10^4	6.52e-22	3.56e-22	3.21e4	n
10	9	11	8	10^4	1.00e-23	8.21e-23	1.07e2	y
10	9	11	10	10^4	1.00e-23	3.92e-24	7.30e4	n
15	7	16	8	10^4	1.54e-22	9.47e-23	4.12e3	n
20	10	21	11	10^4	3.39e-23	2.17e-23	1.08e3	n
25	12	26	13	10^4	1.38e-23	9.39e-24	3.45e2	n
15	7	16	6	10^4	1.54e-22	1.91e-22	3.08e2	y
20	10	21	9	10^4	3.39e-23	4.64e-23	6.37e1	y
10	5	11	4	100	3.45e-20	2.76e-20	2.00e3	y
10	5	11	6	100	3.45e-20	2.68e-20	3.21e4	n
10	5	11	4	10^3	7.59e-21	6.78e-21	2.00e3	y
10	5	11	6	10^3	7.59e-21	5.12e-21	3.21e4	n
10	5	11	4	10^5	2.60e-23	3.30e-23	2.00e3	y
10	5	11	6	10^5	2.60e-23	1.31e-23	3.21e4	n